Biol. Cybern. 89, 81–88 (2003)
DOI 10.1007/s00422-003-0425-7

Biological Cybernetics

Letter to the Editor

A model of desynchronizing deep brain stimulation with a demand-controlled coordinated reset of neural subpopulations

Peter A. Tass

Institute of Medicine, Research Center Jülich, Leo-Brandt-Str., D-52425 Jülich, Germany
Department of Stereotaxic and Functional Neurosurgery, University of Cologne, Joseph-Stelzmann-Str. 9, 50931 Cologne, Germany

Received: 8 November 2002 / Accepted: 9 May 2003 / Published online: 14 July 2003

Abstract. The coordinated reset of neural subpopulations is introduced as an effectively desynchronizing stimulation technique. For this, short sequences of high-frequency pulse trains are administered at different sites in a coordinated way. Desynchronization is easily maintained by performing a coordinated reset with demand-controlled timing or by periodically administering resetting high-frequency pulse trains of demand-controlled length. Unlike previously developed methods, this novel approach is robust against variations of model parameters and does not require time-consuming calibration. The novel technique is suggested to be used for demand-controlled deep brain stimulation in patients suffering from Parkinson's disease or essential tremor. It might even be applicable to diseases with intermittently emerging synchronized neural oscillations like epilepsy.

1 Introduction

In several neurological diseases like Parkinson's disease (PD) or essential tremor, brain function is severely impaired by synchronization processes (Elble and Koller 1990). Parkinsonian resting tremor appears to be caused by a population of neurons located in the thalamus and the basal ganglia. These neurons fire in a synchronized and intrinsically periodical manner at a frequency similar to that of the tremor, regardless of any feedback signals (Llinás and Jahnsen 1982; Pare et al. 1990; Lenz et al. 1994). In contrast, under physiological conditions these neurons fire incoherently (Nini et al. 1995). In patients with PD, this cluster acts like a pacemaker and activates premotor areas and the motor cortex (Alberts et al. 1969; Volkmann et al. 1996), where the latter synchronize their oscillatory activity (Tass et al. 1998).

In patients with advanced PD or essential tremor who no longer respond to drug therapy, depth electrodes are chronically implanted in target areas like the thalamic ventralis intermedius nucleus or the subthalamic nucleus (Benabid et al. 1991; Blond et al. 1992). Electrical deep brain stimulation (DBS) is performed by administering a permanent high-frequency (HF) (> 100 Hz) periodic pulse train via the depth electrodes (Benabid et al. 1991; Blond et al. 1992). HF DBS has been developed empirically, and its mechanism is not yet fully understood. Permanent HF stimulation basically mimics the effect of tissue lesioning by suppressing neuronal firing, which in turn suppresses the peripheral tremor (Wielepp et al. 2001). HF DBS is reversible and has a much lower rate of side effects than lesioning with thermocoagulation (Schuurman et al. 2000). Nevertheless, due to current spread, for example, HF DBS may lead to severe side effects like dysarthria, dysesthesia, or cerebellar ataxia.

For this reason stimulation techniques have been developed that aim at desynchronizing the pacemaker's pathologically synchronized firing in a demand-controlled way instead of by simply suppressing the neuronal firing (Tass 2001a,b,c, 2002a,b,d). These methods share one particular feature: each stimulus consists of two qualitatively different stimuli. The first stimulus is stronger and resets (restarts) the cluster, whereas the second, weaker stimulus is a single pulse that is administered after a constant time delay and desynchronizes by hitting the cluster in a vulnerable state. The goal of the reset is to control the dynamics of the cluster by restarting the cluster in a stereotypical way. The reset may be achieved by means of a strong single pulse (Tass 2001a,c, 2002d), a HF pulse train (Tass 2001b), or a low-frequency pulse train (Tass 2002a,b).

A desynchronizing single pulse is effective only if it hits the population very precisely at a vulnerable phase (Tass 1999). Hence the composite stimulation techniques only work with an effective reset that may require high stimulation intensities, and minor variations of critical stimulation parameters (especially the delay between resetting stimulus and desynchronizing single pulse) may abolish the desynchronizing effect (Tass 2001c, 2002b). Thus these methods are not robust against larger variations of the model parameters (frequencies of the

Correspondence to: Peter A. Tass
(e-mail: P.Tass@fz-juelich.de)

neurons and strength of synaptic interactions). Furthermore, these techniques require a time-consuming calibration procedure lasting more than 30 min (based on series of test stimuli) (Tass 1999). Unlike resetting stimuli, the desynchronizing methods have not yet been sufficiently tested during operation. They will be tested after operation in selected patients with an external connection to their implanted electrodes. In summary, the previous methods can only be applied to synchronized oscillations if their dynamical features are reasonably stable and if there is enough time for calibration.

In this paper, these difficulties are surmounted by separately stimulating subpopulations. A coordinated reset of neural subpopulations with demand-controlled timing or with demand-controlled length of periodically administered HF pulse trains causes, in my model, an effective desynchronization. These novel techniques are robust with respect to variations of model parameters, and there is no need for time-consuming calibration. Their robustness and rapid availability make the novel stimulation techniques clearly superior to the previously developed methods. The novel methods should be tested in patients with advanced PD or essential tremor and might even be applicable to diseases with intermittently emerging synchronized neural oscillations like epilepsy.

2 Model

The dynamics of a neuronal population can be modeled with a network of phase oscillators (Kuramoto 1984; Ermentrout and Kopell 1991; Grannan et al. 1993; Hansel et al. 1993). The population of N interacting phase oscillators subject to stimulation and to random forces obeys

$$\dot{\psi}_j = \Omega - \frac{K}{N}\sum_{k=1}^{N}\sin(\psi_j - \psi_k) + X_j(t)S_j(\psi_j) + F_j(t) \qquad (1)$$

where ψ_j denotes the phase of the jth phase oscillator. All oscillators have the same eigenfrequency Ω and are globally coupled with strength $K > 0$. In neurons, the impact of an electrical stimulus depends on the neuron's phase (Best 1979; Guttman et al. 1980). Hence the stimulus is modeled by a 2π-periodic function like $S_j(\psi_j) = I\cos\psi_j$ with intensity parameter I.

$$X_j(t) = \begin{cases} 1: & \text{neuron } j \text{ is stimulated at time } t \\ 0: & \text{else} \end{cases} \qquad (2)$$

takes into account switching on and off stimulation of the jth oscillator. The random forces $F_j(t)$ are Gaussian white noise with $\langle F_j(t)\rangle = 0$ and $\langle F_j(t)\ F_k(t')\rangle = D\delta_{jk}\ \delta(t-t')$, where D is the constant noise amplitude. For vanishing stimulation ($X = 0$), Eq. 1 is a well-known standard model of coupled phase oscillators (Kuramoto 1984). Compared to a previously introduced model for a homogenously stimulated population of phase oscillators (with $S_j = S_k$ for $j,k = 1,\ldots,N$) (Tass 1999), Eq. 1 takes into account that different oscillators may be stimulated differently.

3 Coordinated reset of neural subpopulations

A phase-dependent stimulus, like $S_j(\psi_j) = I_j\cos(\psi_j)$, resets the jth oscillator to a particular phase if the intensity parameter I_j is large compared to the coupling strength and to the noise amplitude and provided the stimulation duration is long enough (Tass 1999, 2002c). Such a reset can be achieved with a strong single pulse (Tass 1999, 2001a, 2002d), a HF pulse train (with a pulse rate 20 times larger than the mean eigenfrequency Ω) (Tass 2001b) or a low-frequency pulse train (with a pulse rate similar to Ω) (Tass 2002a,b). Here we use a HF pulse train for the reset.

First, let us assume that there is no noise ($D = 0$). A HF pulse train with $S_j(\psi_j) = I_j\cos(\psi_j + \theta)$ resets the jth neuron close to the phase $\psi_j^{\text{res}} + \theta$ (Tass 1999, 2002c). Thus, we could easily desynchronize the population by stimulating each neuron separately to achieve equidistant resets. For this, we would administer HF pulse trains of identical timing (i.e., $X_j(t) = X(t)$ for $j = 1,\ldots,N$) but different stimulation mechanisms $S_j(\psi_j) = I_j\cos[\psi_j + 2\pi(j-1)/N]$. After stimulation the population would be perfectly desynchronized, with a uniform distribution of the phases $\psi_j^{\text{res}} + 2\pi(j-1)/N$. However, stimulating each neuron separately would require the use of many electrodes and would easily damage or even destroy the neural tissue. Furthermore, noise makes the reset less perfect: the jth phase after stimulation would be $\psi_j^{\text{res}} + 2\pi(j-1)/N + \xi_j$ with a deviation ξ_j due to noise. Therefore, we choose a different goal. Instead of forcing the population into a state with a perfectly uniform distribution of the phases, we simply split the population into a few, say four, subpopulations equally spaced in a cycle $[0, 2\pi]$.

We denote as *subpopulations* 1, 2, 3, and 4 the groups of neurons $j = 1,\ldots,N/4$, $j = N/4+1,\ldots,N/2$, $j = N/2+1,\ldots,3N/4$, and $j = 3N/4+1,\ldots,N$, respectively (with N divisible by 4). To split the population in four equally spaced subpopulations we may choose qualitatively different strategies. (i) *Simultaneous stimulation* of all four subpopulations: phase shifts of the reset neurons are induced by phase shifts of the stimulation mechanisms. We may stimulate neuron j of subpopulation $k = 1,\ldots,4$ with a HF pulse train with $S_j(\psi_j) = I\cos[\psi_j + 2\pi(k-1)/4]$. (ii) The four subpopulations are *stimulated at different times with identical stimulation mechanisms* S_j. The delay between subsequent HF pulse trains is equal to $T/4$, where $T = 2\pi/\Omega$ is the period of the population without stimulation. We may stimulate neuron j of subpopulation $k = 1,\ldots,4$ at time $t' + T(k-1)/4$ with a HF pulse train with $S_j(\psi_j) = I\cos(\psi_j)$. (iii) Strategies (i) and (ii) can be combined, e.g., by performing *two subsequent antiphase resets of pairs of subpopulations with a time delay of* $T/4$ (Fig. 1a). Subpopulation 1 and 2 are stimulated simultaneously at time t' but with different polarity. A neuron of subpopulation 1 is stimulated with $S_j(\psi_j) = I\cos(\psi_j)$, whereas a neuron of subpopulation 2 is stimulated with $S_j(\psi_j) = I\cos(\psi_j + \pi) = -I\cos(\psi_j)$. Analogously, subpopulations 3 and 4 are simultaneously stimulated at time $t' + T/4$. A neuron of subpopulation 3 is stimulated

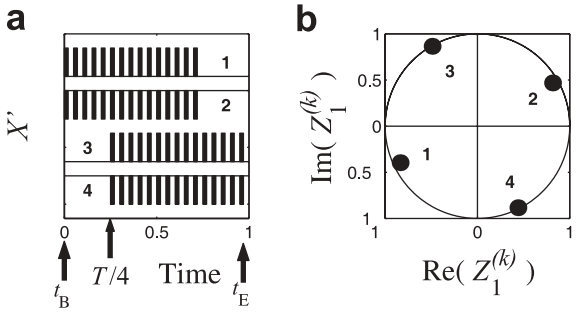

Fig. 1. **a** Two subsequent antiphase resets of pairs of subpopulations are achieved by administering two pairs of high-frequency (HF) pulse trains with different polarity with a time delay of $T/4$, where $T = \Omega/(2\pi)$ is the period of the population. Time course and polarity of HF pulse trains is schematically indicated with $X'(t) = X(t)S_j(0)$, where the *numbers* indicate the subpopulation to which the corresponding HF pulse train is administered. Single pulses are highlighted by *shaded regions*. Each HF pulse train consists of 15 single pulses with duration 0.02 intersected by pauses of length 0.03. HF pulse trains 1 and 3 have positive polarity, $S_j(\psi_j) = I\cos(\psi_j)$, whereas HF pulse trains 2 and 4 have negative polarity, $S_j(\psi_j) = -I\cos(\psi_j)$, with $I = 30$. Stimulation starts at time $t_B = 0$ and ends at $t_E = 0.97$. **b** Stimulating Eq. 1 according to **(a)** results in a configuration at the end of the stimulation given by $Z_1^{(k)}(t_E)$, where *numbers* indicate the corresponding subpopulation $k = 1, \ldots, 4$. The *unit circle* marks the maximal range of $|Z_1^{(k)}|$. Model parameters: $N = 100$, $K = 2$, $\Omega = 2\pi$, noise amplitude $D = 0.4$

with $S_j(\psi_j) = I\cos(\psi_j)$, whereas a neuron of subpopulation 4 is stimulated with $S_j(\psi_j) = -I\cos(\psi_j)$.

Variants (i)–(iii) work comparably well. Due to space restrictions, only version (iii) will be demonstrated. To estimate the extent and type of synchronization of the whole population, we use the cluster variables

$$Z_m(t) = R_m(t)e^{\mathrm{i}\varphi_m(t)} = \frac{1}{N}\sum_{j=1}^{N} e^{\mathrm{i}m\psi_j(t)} \tag{3}$$

where $R_m(t)$ and $\varphi_m(t)$ are the corresponding real amplitude and real phase, where $0 \le R_m(t) \le 1$ for all times t (Daido 1992; Tass 1999). Cluster variables are convenient for characterizing synchronized states of different type: perfect in-phase synchronization corresponds to $R_1 = 1$, whereas an incoherent state, with uniformly distributed phases, is associated with $R_m = 0$ $(m = 1, 2, 3, \ldots)$. $R_1 = 0$ combined with large R_m is indicative of an m-cluster state consisting of m distinct and equally spaced clusters, where within each cluster all oscillators have similar phase. Analogously, we use

$$Z_m^{(k)}(t) = R_m^{(k)}(t)e^{\mathrm{i}\varphi_m^{(k)}(t)} = \frac{4}{N}\sum_{j\in\Lambda_k} e^{\mathrm{i}m\psi_j(t)} \tag{4}$$

as cluster variables for the four subpopulations separately. $k = 1, \ldots, 4$ is the index of the subpopulation introduced above, m is the index referring to an m-cluster state (Eq. 3), and Λ_k is the set of indices belonging to the kth subpopulation, e.g., $\Lambda_1 = \{1, \ldots, N/4\}$. With $Z_1^{(k)}$ we estimate the extent of in-phase synchronization within subpopulation k. The latter is perfectly in-phase synchronized if $R_1^{(k)} = 1$.

The effect of the coordinated reset is visualized in Fig. 1b by showing a snapshot of $Z_1^{(k)}(t_E)$, the centers of mass of all four subpopulations at the end of the stimulation. All four subpopulations are strongly synchronized, where their mean phases $\varphi_1^{(k)}$ are equally spaced in the cycle. $R_1^{(1)}$ and $R_1^{(2)}$ are slightly smaller than $R_1^{(3)}$ and $R_1^{(4)}$. This follows from the fact that at the end of HF pulse trains 1 and 2 (i.e., at time $t_E - T/4$) $Z_1^{(1)}$ and $Z_1^{(2)}$ are located exactly where $Z_1^{(3)}$ and $Z_1^{(4)}$ are located at the end of HF pulse trains 3 and 4 (i.e., at the end of the stimulation, at time t_E). Between $t_E - T/4$ and t_E subpopulations 1 and 2 spontaneously run in counterclockwise direction through a quarter of a cycle and relax to a less synchronized state with smaller $R_1^{(1)}$ and $R_1^{(2)}$. The arrangement of $Z_1^{(1)}, \ldots, Z_1^{(4)}$ at the end of the stimulation is a symmetrical four-cluster state of the whole population, with R_4 from Eq. 3 close to 1 and R_1 close to 0. The coordinated reset splits the whole populations in four distinct, symmetrically arranged subpopulations.

4 Effective desynchronization

To understand how a stimulus-induced clustering leads to an effective desynchronization, we have to study the dynamics of the leading modes $Z_1, \ldots, Z_4$. We first recall the dynamical behavior of Eq. 1 without stimulation (with $X(t) = 0$ in Eq. 2). For large N it has been shown that noisy in-phase synchronization emerges out of the incoherent state due to a decrease of the noise amplitude D (Kuramoto 1984) or, analogously, because of an increase of the coupling strength (Tass 1999). For $K > D$ a stable limit cycle $Z_1(t) = Y\exp(i\Omega t)$ emerges, where Y is a complex constant (Tass 1999). When K exceeds its critical value $K^{\mathrm{crit}} = D$, Z_1 from Eq. 3 becomes an *order parameter*, which according to the slaving principle (Haken 1983) governs the dynamics of the other, stable modes Z_m $(m = 2, 3, \ldots)$ on the center manifold (Pliss 1964): the order parameter Z_1 acts on a slow time scale, whereas the stable modes Z_m act on a fast time scale and relaxes to values given by the order parameter Z_1 (Wunderlin and Haken 1975; Haken 1983). In Eq. 1 with large N, this relationship reads (Tass 1999):

$$R_m \propto R_1^{\nu} \quad \text{with} \quad \nu \ge 2,\ m = 2, 3, 4, \ldots \tag{5}$$

The collective dynamics will be visualized not only with the cluster variables Z_m but also by considering the collective firing. A single firing/bursting model neuron fires/bursts whenever its phase is close to zero (modulo 2) (Kuramoto 1984; Ermentrout and Kopell 1991; Grannan et al. 1993; Hansel et al. 1993; Tass 1999). The cluster's collective firing activity is given by the *relative number of neurons producing an action potential or burst*:

$$n_{\mathrm{fire}}(t) = \frac{\text{number of neurons with } \cos\psi_j > 0.99}{N} \tag{6}$$

$0 \le n_{\mathrm{fire}}(t) \le 1$ for all t. Varying the threshold parameter 0.99 in a reasonable range does not change the results.

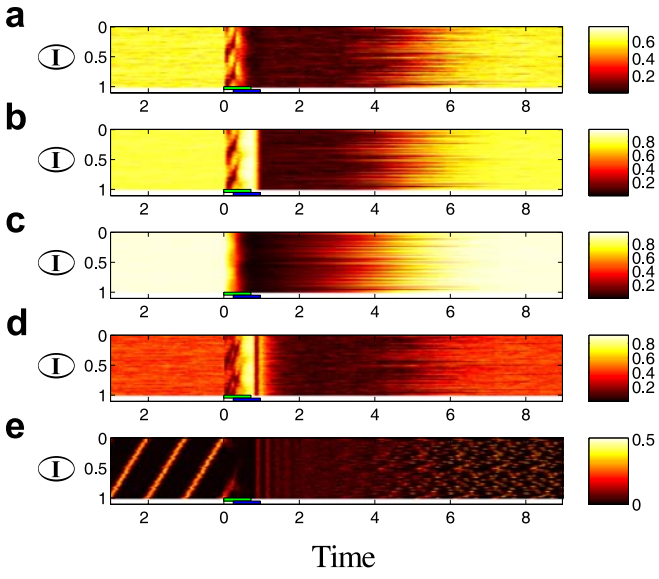

Fig. 2a–e. The stimulus from Fig. 1a is administered to the in-phase synchronized neuronal population from Eq. 1 at different initial phases. At the beginning of each simulation the phases are given by $\psi_j = \Psi + \Delta\psi_j$, where $\Delta\psi_j$ is normally distributed with variance $\sqrt{0.3}$. The time course of R_1 (**a**), R_2 (**b**), R_3 (**c**), R_4 (**d**) from Eq. 3 and the relative number of firing neurons n_{fire} from Eq.6 (**e**) is shown in 101 simulations, where the normalized mean initial phase $\Theta = \Psi/(2\pi)$ is varied in equidistant steps within one cycle $[0, 1]$. Equation 1 is integrated with Euler's technique with a time step of 0.0001. The first 30,000 time steps were discarded to guarantee that the stimuli hit the population in a stable synchronized state. Same stimulation parameters and model parameters as in Fig. 1. Stimulation starts at $t_B = 0$ and ends at $t_E = 0.97$. Pairs of HF pulse trains 1, 2 and 3, 4 are indicated by *green* and *blue horizontal bars*, respectively

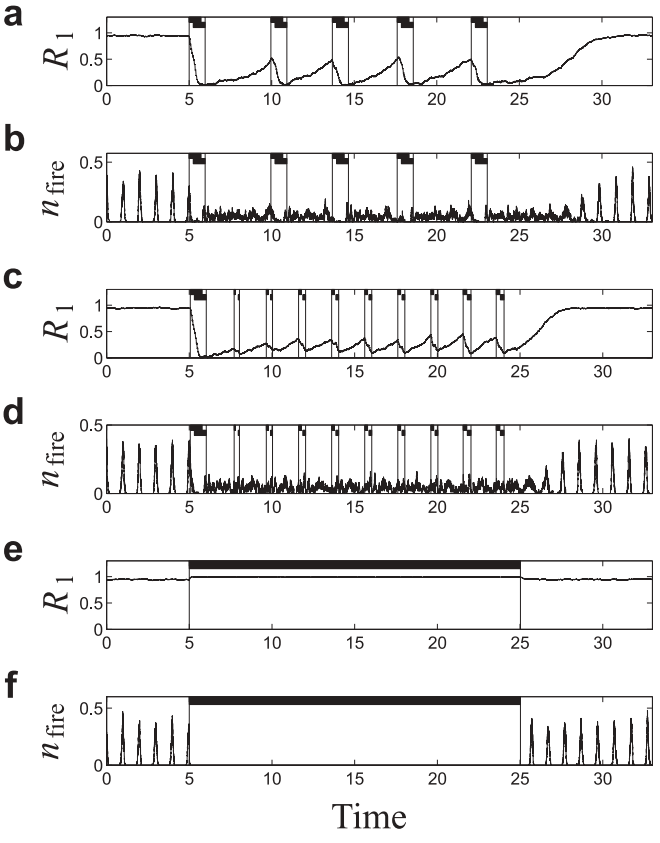

Fig. 3. Time course of R_1 from Eq. 3 (**a**, **c**, **e**), and of n_{fire} from Eq. 6 (**b**, **d**, **f**) during different types of stimulation. *Demand-controlled timing of stimulus administration* (**a**, **b**): As soon as the amplitude R_1 of the recovering order parameter reaches the value of 0.5, the stimulus from Fig. 1a is administered again. *Periodical stimulation with demand-controlled length of HF pulse train* (**c**, **d**): The stimulus from Fig. 1a is administered periodically, where the length of the HF pulse trains is adapted to R_1 according to Eq. 7 with $M_{\max} = 15$ and $M_{\min} = 0$. *Standard permanent HF pulse train stimulation* (**e**, **f**): Each neuron is stimulated with the same HF pulse train: $X_j(t) = X(t)$ in Eqs. 1 and 2. **a**–**f**: Numerical integration, model parameters, and initial conditions as in Fig. 2. Beginning and end of stimuli are indicated by *vertical lines*. **a**–**d**: Upper and lower *shaded regions* correspond to pairs of HF pulse trains 1, 2 and 3, 4, respectively. **e**, **f**: HF pulse train is indicated by one *shaded region*

$n_{\text{fire}}(t) = 0$ means that no neuron fires/bursts, while all neurons fire/burst at time t if $n_{\text{fire}}(t) = 1$.

Figure 2 shows the dynamics before, during, and after stimulation. The phase at which the coordinated reset from Fig. 1 is applied to the same neuronal population is varied within one cycle. The impact of this stimulus is independent of the phase at which it is administered. At the end of the stimulation the system has reached the four-cluster state shown in Fig. 1a: R_4 has a value similar to the prestimulus range, whereas R_1, R_2, and R_3 are close to zero. In the poststimulus period, the system does not remain in the four-cluster state. Rather, due to the slaving principle, R_4 rapidly decays to zero, so that the system approaches a perfectly desynchronized state characterized by $R_m = 0$ ($m = 1, 2, 3, 4, \ldots$). The vanishing R_1 suppresses R_4 according to Eq. 5. Without coupling (but with noise) the four-cluster state would decay more slowly (see (Tass 1996)).

From the mathematician's viewpoint the relaxation of R_4 is due to the system being attracted by the center manifold as characterized by Eq. 5. By imposing a four-cluster state, the stimulation does only half of the desynchronizing work. The rest, namely, approaching a uniformly desynchronized state, is done by the system itself. In this way, the coupling, which causes the synchronization, is used for improving the desynchronizing effect. In the course of the poststimulus transient R_1 and according to Eq. 5, R_2, R_3, and R_4 also recover again. The system finally reaches its stable in-phase synchronized state again. The results are stable with respect to variations of N between 20 and 1000 and more.

5 Block of resynchronization

The effectively desynchronizing coordinated reset of subpopulations can be used to block the resynchronization. For this, we may use two different strategies:

(i) *Demand-controlled timing of the administration of identical stimuli*. Whenever the population tends to resynchronize, the same stimulus is administered (Fig. 3). The larger the coupling strength K, the more often a stimulus has to be administered to maintain an uncorrelated firing. In an experimental application, one has to

observe the synchronized oscillation during a sufficiently long period of time in order to perform a frequency analysis that yields the period T of the population in the absence of stimulation and, thus, the critical stimulation parameter $T/4$ (the time delay between the two pairs of HF pulse trains, Fig. 1a).

(ii) *Entrainment with periodically administered HF pulse trains of demand-controlled length*. The stimuli are periodically administered with offset times $t_n = nv\tau$, where $n = 0, 1, 2, 3, \ldots$ is the index labeling the various stimuli, $\tau = T + \varepsilon$ is a time interval in the range of the period T of the population without stimulation, and v is a small integer such as 2 or 3. This means we perform a $1 : v$ entrainment of the four subpopulations, where the spontaneous frequency of the neurons is approximately v times larger compared to the frequency of stimulus administration. The smaller $|\varepsilon|$, the smaller is the stimulation strength necessary to achieve an entrainment.

Unlike in Sect. 3 (Fig. 1a), we use HF pulse trains of demand-controlled length: the length of the HF pulse trains increases linearly between a minimal value $M_{\min}$ and a maximal value $M_{\max}$ of single pulses (except for rounding), where the latter is initially used for desynchronizing the fully synchronized population. R_1 is measured at times $t'_n = t_n - t_{\max}$, where $t_{\max}$ is the maximal duration of a HF pulse train (containing $M_{\max}$ single pulses). $R_1(t'_n)$ determines the number of pulses of the HF pulse trains 1–4 of the nth stimulus according to

$$M_n = \min\left\{\left[\frac{R_1(t'_n)(M_{\max}-M_{\min})}{R_1(t_0)}\right]_{\mathbb{Z}} + M_{\min}, M_{\max}\right\} \tag{7}$$

where $n = 0, 1, 2, 3, \ldots$, $[x]_{\mathbb{Z}}$ stands for rounding x to the nearest integer, and $\min\{x_1, x_2\}$ stands for the minimum of $\{x_1, x_2\}$. The nth stimulus ends precisely at time $t_n = nv\tau$, whereas it starts somewhere between t'_n (for $M_n = M_{\max}$) and t_n (for $M_n = M_{\min} = 0$), depending on its duration. With this adaptive entrainment we stabilize the periodic motion of $Z_1^{(1)}, \ldots, Z_1^{(4)}$, the centers of mass of the four subpopulations. In this way, only minor corrections are necessary to keep the centers of mass $Z_1^{(1)}, \ldots, Z_1^{(4)}$ sufficiently close to their corresponding attractors (Fig. 1a) at times $t_n = nv\tau$. If the suppression of R_1 is not sufficient, we may (i) choose a larger intensity parameter I in $S_j(\psi_j) = I\cos\psi_j$, (ii) increase $M_{\min}$, (iii) administer the stimuli at a higher rate, i.e., decrease v so that the interstimulus interval $t_{n+1} - t_n = v\tau$ gets smaller, and/or (iv) increase the duration of each single pulse of the pulse trains. The feedback value of R_1 can also be evaluated before time t'_n, especially in case of a slow order parameter dynamics (i.e., when the coupling is weak with respect to the noise). We could also use the mean of R_1 in a period of evaluation.

Applying the standard, permanent HF pulse train stimulation (Benabid et al. 1991; Blond et al. 1992) to our Eq. 1 (in a first approximation) corresponds to stimulating each neuron with the same HF pulse train [$X_j(t) = X(t)$ in Eqs. 1 and 2]. During a permanent HF stimulation a high-frequency entrainment of the order parameter Z_1 captures Z_1 in a small portion of the Gaussian plane (Tass 2001b), so that the individual neurons' firing is stopped, but no desynchronization occurs (Fig. 3e,f). In contrast, during stimulation R_1 is larger compared to its prestimulus level, and after stimulation the synchronous firing continues immediately. To suppress the firing with such a simple pulse train persistently, it has to be administered permanently. The number of single pulses used to suppress the firing in Fig. 3e,f is 5.35 and 8.02 times larger than that used for blocking the resynchronization in Figs. 3a,b and 3c,d, respectively.

6 Demand-controlled deep brain stimulation

I suggest using the demand-controlled stimulation techniques shown in Fig. 3a–d for the therapy of neurological diseases like Parkinson's disease or essential tremor. The demand-controlled stimulation techniques may be realized technically in different ways by using several electrodes or an electrode with several contacts. The main point is to achieve a coordinated reset of neural subpopulations central to the pathological dynamics.

For the feedback control of the stimulation we need a signal reflecting the extent of synchronization within the target population (corresponding to R_1 in Fig. 3). This signal may be a local field potential (LFP) measured via the electrodes used for stimulation. Alternatively, we may use an epicortical electrode measuring the electrical activity in cortical areas that are sufficiently strongly synchronized with the target area stimulated via the depth electrodes (e.g., premotor areas, primary motor cortex). A desynchronizing coordinated reset (Fig. 1a) is performed either with a demand-controlled timing (Fig. 3a,b) or periodically with a demand-controlled length of the HF pulse train (Fig. 3c,d). The goal of this approach is to effectively block the resynchronization and, hence, keep the firing as close as possible to the physiological (i.e., uncorrelated) firing mode.

To illustrate how a coordinated reset of different parts of a target population is achieved by simply stimulating at four different sites (Fig. 4b), we model the impact of the four stimulating electrodes on the jth neuron by

$$X_j(t)S_j(\psi_j) = \sum_{k=1}^{4} Y_k(t) I\cos(\psi_j)\rho_j^{(k)} \tag{8}$$

where k is the index referring to the electrode. The time course of the HF pulse train administered via the kth electrode is given by Y_k. It is identical to the kth HF pulse train shown in Fig. 1a. Y_k is 0 when there is no stimulation and $+1$ or -1 else, depending on the polarity of the electrode. HF pulse trains 1 and 2 as well as 3 and 4 have opposite polarity: $Y_1 = -Y_2$, $Y_3 = -Y_4$, where HF pulse trains 3 and 4 are delayed by $T/4$. The influence of the kth electrode on the jth neuron is modeled by $I\cos(\psi_j)$ as in the simulations of Figs. 1–3. The effect of stimulation decays with increasing distance between neuron and electrode, where the spatial activation

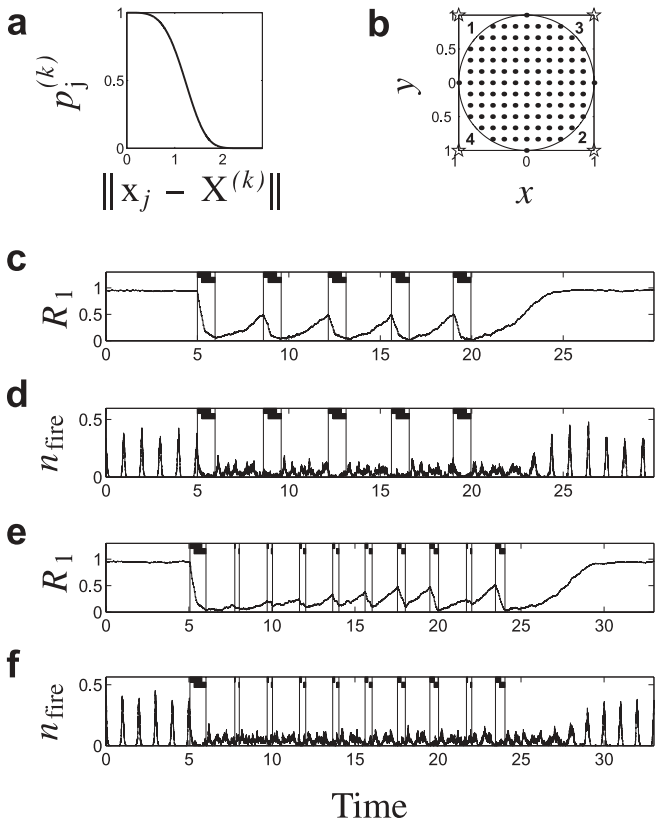

Fig. 4. **a** The effect of the kth electrode on the jth neuron, $\rho_j^{(k)} = \exp[(-0.75 * \|\mathbf{x}_j - \mathbf{X}^{(k)}\|)^4]$, decays with increasing distance between neuron and electrode $\|\mathbf{x}_j - \mathbf{X}^{(k)}\|$. **b** 113 neurons (*dots*) are placed on a grid within the unit circle. The four stimulation electrodes (indicated by *stars* labeled by *numbers*) are placed at the corners of the unit square. Time courses of R_1 from Eq. 3 (**c**, **e**) and of n_{fire} from Eq. 6 (**d**, **f**). As in Fig. 3a–d, demand-controlled stimulation techniques are applied, where four different HF pulse trains (modeled by $Y_k(t)$ in Eq. 8 and shown in Fig. 1a) are administered via the four electrodes from **b**, respectively. *Demand-controlled timing of stimulus administration* (**c**, **d**): as soon as $R_1 = 0.5$, the next stimulus is administered. *Periodical stimulation with demand-controlled length of HF pulse train* according to Eq. 7, where $M_{\max} = 15$ and $M_{\min} = 0$ (**e**, **f**). **c**–**f** Model parameters, initial conditions, and format as in Fig. 3, except for $I = 40$ (used for compensating for the decay of $\rho_j^{(k)}$)

profile is not known in detail (Ranck 1975). We model the ring-type distance dependence by $\rho_j^{(k)} = \exp[(-a * \|\mathbf{x}_j - \mathbf{X}^{(k)}\|)^b]$ with $a = 0.75$ and $b = 4$ (see Figs. 1 and 2 in Ranck 1975). Results are qualitatively invariant with respect to variations of a between 0.25 and 0.75 and b between 2 and 6.

Both a demand-controlled timing of the stimulus administration (Fig. 4c,d) and a periodical stimulation with demand-controlled length of the HF pulse trains (Fig. 4e,f) effectively desynchronize the target population.

7 Discussion

Novel, effectively desynchronizing stimulation techniques are presented: a coordinated reset of neural subpopulations with demand-controlled timing (Fig. 3a,b) or with demand-controlled length of periodically administered HF pulse trains (Fig. 3c,d). Applied to Eq. 1 these methods work very well and are superior to permanent HF pulse train stimulation, the standard method for DBS (Benabid et al. 1991; Blond et al. 1992): permanent HF stimulation simply suppresses the firing (Fig. 3e,f), whereas the novel techniques desynchronize it and, thus, bring it close to the physiological mode (Fig. 3a–d). Moreover, the energy consumption of the novel methods is considerably smaller (Sect. 5). This difference is even more pronounced in the case of realistic (i.e., weaker) coupling, when it takes the population much longer to resynchronize. In this paper, rather strong coupling has been used for the sake of clearness.

Compared to previously developed demand-controlled techniques that act on a population homogenously (with $S_j = S_k$ for $j, k = 1, \ldots, N$ in Eq. 1) (Tass 2001a,b,c, 2002a,b,d), the novel techniques presented here may have a slightly larger energy consumption when applied to Eq. 1. For a decrease of the firing by 70% the previous techniques require 8.82, 8.11, and 4.25 times less energy compared to standard permanent HF stimulation, provided the reset is achieved with a strong pulse, a HF pulse train, and a low-frequency pulse train, respectively (Tass 2002b). These ratios were determined for Eq. 1 with $N \to \infty$, where N is the number of oscillatory neurons. In contrast, the corresponding ratios of the novel methods read 5.35 for demand-controlled timing and 8.02 for demand-controlled length of HF pulse trains and were determined with $N = 100$ (Sect. 5). Because of the different values of N, comparisons of the different ratios have to be drawn cautiously. A detailed comparison of the energy consumption will be presented soon.

The absence of critical stimulation parameters, the robustness of the desynchronizing effect, and the quick availability (without time-consuming calibration) make the novel stimulation techniques, in particular the periodical stimulation with demand-controlled length of the HF pulse trains (Figs. 3c,d and 4e,f), superior to the previously developed demand-controlled techniques that act on a population homogenously (Tass 2001a,b,c, 2002a,b,d). Concerning the effects on Eq. 1, periodical stimulation with demand-controlled length of the HF pulse trains (Fig. 3c,d) is more powerful compared to the demand-controlled timing of the stimuli (Fig. 3a,b):

1. The demand-controlled adaptation of the length of the HF pulse trains needs less energy: during the entrainment $Z_1^{(1)}, \ldots, Z_1^{(4)}$, the centers of mass of the four subpopulations run in counterclockwise direction along the unit circle. After two cycles ($v = 2$) we control whether they are equally spaced, as shown in Fig. 1a. The more their arrangement deviates from this perfect four-cluster state, the more often we kick the subpopulations toward their attractors. The larger the distance between $Z_1^{(k)}$ and its corresponding attractor, the longer the chosen HF pulse train has to be in order to move $Z_1^{(k)}$ close to its attractor (Tass 2001b). A stable entrainment guarantees that we need only short HF pulse trains to

perform minor corrections of the periodic trajectories of $Z_1^{(1)}, \ldots, Z_1^{(4)}$. We use the inner tendency of the neurons to be active periodically in order to save stimulation energy. In contrast, if we administer a long HF pulse train whenever the amplitude of the order parameter R_1 exceeds a critical value (Fig. 3a,b), $Z_1^{(1)}, \ldots, Z_1^{(4)}$ may be far away from their corresponding attractors, so that short HF pulse trains are not sufficient.

2. The demand-controlled adaptation of the length of the HF pulse trains can be applied without a preceding time-consuming frequency analysis. In an experimental application, the time delay between HF pulse trains 1 and 2 on the one hand and HF pulse trains 3 and 4 on the other hand is simply chosen to be a quarter of τ, the period of the entrained oscillation, instead of a quarter of T, the period of the spontaneous oscillation (Fig. 1a and Sect. 4). By entraining the neural population with a periodical stimulation, we know the right value of the time delay between the HF pulse trains from the very beginning, since we dictate τ, the period of the entrained oscillation. The consequences are obvious. (i) The periodical stimulation with demand-controlled length of HF pulse trains is much more robust with respect to variations of the eigenfrequencies of the neurons. (ii) This stimulation method does not require a time-consuming calibration. It may, thus, even be used to quickly react on intermittently emerging synchronized neural oscillations, provided the typical frequency range is known approximately. Accordingly, this stimulation might also be beneficial to patients suffering from epilepsy.

A demand-controlled adaptation of the intensity I (as opposed to a demand-controlled adaptation of the length of the HF pulse trains) would not lead to a comparably effective desynchronization. Decreasing I may change the attractor of a single pulse drastically, and instead of stable fixed points (Fig. 1b) qualitatively different attractors like limit cycles may occur (Tass 1999, 2001c). A demand-controlled intensity I would lead to a hopping between qualitatively different attractors.

Already in the late 1950s it was shown that Parkinsonian tremor is entrained by periodic DBS of the pallidum at rates similar to the peripheral tremor frequency (Hassler et al. 1960). A desynchronization by means of a coordinated entrainment of neural subpopulations (Fig. 3c,d) has not yet been applied.

The desynchronizing effect of directly stimulating the target population at four different sites (Fig. 4) is stable with respect to variations of the spatial position of the stimulation electrodes, at least in the model. Asymmetries of the spatial arrangement can be compensated for by adjusting the intensity parameter I for the different electrodes separately: the smaller the rhythmic component of the measured LFP, the stronger the chosen intensity parameter has to be for this particular electrode. With the simple spatial electrode arrangement shown in Fig. 4b the four subpopulations cannot be stimulated in a perfectly separate way. Therefore, the second mode (R_2 from Eq. 3 of the population is not completely suppressed after stimulation, not shown due to space constraints; cf. Figs. 2, 3), and the extent of uniform desynchronization is smaller. As an alternative to a direct stimulation of the target population, we might stimulate the target population indirectly by stimulating different parts of fiber connections or different brain areas projecting on different parts of the target population.

A similar order parameter-driven rapid relaxation of excited stable modes (Sect. 4) has already been studied in detail in the context of dynamical side effects of spatially homogenous stimulation techniques (with $S_j = S_k$ for $j, k = 1, \ldots, N$; Sect. 6.2.3 in (Tass 1999)): the larger m, the faster an excited mth mode relaxes. For this reason a separate stimulation of four subpopulations has been chosen here. In contrast, separately stimulating only two subpopulations would not yield the desired effect, since the second mode decays too slowly, so that no uniform desynchronization occurs. Separately stimulating three subpopulations is already clearly better, and the separate stimulation of four subpopulations is a sufficient compromise between perfect uniform desynchronization and the use of a minimal number of electrodes (necessary to prevent tissue damage and especially bleeding). A coordinated reset of more than four subpopulations is performed similarly as explained above. For instance, to desynchronize by resetting six subpopulations, we may administer three pairs of HF pulse trains (of opposite polarity) separated by time delays of $\tau/6$, where τ is the period of the entrained collective oscillation (cf. Fig. 1a).

An effective desynchronization only requires the stimulus to be strong enough to suppress the order parameter at the end of the stimulation. The stronger the stimulus, the stronger the excitation of the fourth mode, and the longer it takes R_4 to relax to zero (Sect. 4). Hence increasing the stimulation strength far beyond values sufficient for suppressing the order parameter may counteract desynchronization.

The stimulation techniques presented here also work (i) if both eigenfrequencies and coupling constants are not homogenous but vary within the population ($\Omega \to \omega_j$ and $K \to K_{j,k}$ in Eq. 1) and (ii) if the stimulation mechanism contains higher-order terms like $I_2 \cos(2\psi_j)$. Alternatively, to perform a coordinated reset, we can replace the HF pulse trains by strong single pulses. Future studies will be dedicated to modeling both the neuronal dynamics and the stimulation mechanism on a more microscopic level.

Acknowledgements. This study was supported by the German-Israeli Foundation for Scientific Research and Development (Grant No. 667/00).

References

Alberts WW, Wright EJ, Feinstein B (1969) Cortical potentials and parkinsonian tremor. Nature 221: 670–672

Benabid AL, Pollak P, Gervason C, Hoffmann D, Gao DM, Hommel M, Perret JE, De Rougemont J (1991) Long-term suppression of tremor by chronic stimulation of the ventral intermediate thalamic nucleus. The Lancet 337: 403–406

Best EN (1979) Null space in the Hodgkin–Huxley equations: a critical test. Biophys J 27: 87–104

Blond S, Caparros-Lefebvre D, Parker F, Assaker R, Petit H, Guieu J-D, Christiaens J-L (1992) Control of tremor and involuntary movement disorders by chronic stereotactic stimulation of the ventral intermediate thalamic nucleus. J Neurosurg 77: 62–68

Daido H (1992) Order function and macroscopic mutual entrainment in uniformly coupled limit-cycle oscillators. Prog Theor Phys 88: 1213–1218

Elble RJ, Koller WC (1990) Tremor. John Hopkins University Press, Baltimore

Ermentrout GB, Kopell N (1991) Multiple pulse interactions and averaging in systems of coupled neural oscillators. J Math Biol 29: 195–217

Grannan ER, Kleinfeld D, Sompolinsky H (1993) Stimulus-dependent synchronization of neuronal assemblies. Neural Comp 4: 550–569

Guttman R, Lewis S, Rinzel J (1980) Control of repetitive firing in squid axon membrane as a model for a neurone oscillator. J Physiol (London) 305: 377–395

Haken H (1983) Advanced Synergetics. Springer, Berlin Heidelberg New York

Hansel D, Mato G, Meunier C (1993) Phase dynamics of weakly coupled Hodgkin–Huxley neurons. Europhys Lett 23: 367–372

Hassler R, Riechert T, Mundinger F, Umbach W, Ganglberger JA (1960) Physiological observations in stereotaxic operations in extrapyramidal motor disturbances. Brain 83: 337–350

Kuramoto Y (1984) Chemical Oscillations, Waves, and Turbulence. Springer, Berlin Heidelberg New York

Lenz FA, Kwan HC, Martin RL, Tasker RR, Dostrovsk JO, Lenz YE (1994) Single unit analysis of the human ventral thalamic nuclear group. Tremor-related activity in functionally identfied cells. Brain 117: 531–543

Llinás R, Jahnsen H (1982) Electrophysiology of mammalian thalamic neurons in vitro. Nature 297: 406–408

Nini A, Feingold A, Slovin H, Bergman H (1995) Neurons in the globus pallidus do not show correlated activity in the normal monkey, but phase-locked oscillations appear in the MPTP model of parkinsonism. J Neurophysiol 74(4): 1800–1805

Pare D, Curro'Dossi R, Steriade M (1990) Neuronal basis of the parkinsonian resting tremor: a hypothesis and its implications for treatment. Neuroscience 35: 217–226

Pliss V (1964) Principal reduction in the theory of stability of motion. Izv Akad Nauk SSSR Math Ser 28: 1297–1324

Ranck JB (1975) Which elements are excited in electrical stimulation of mammalian central nervous system: A review. Brain Res 98: 417–440

Schuurman PR, Bosch DA, Bossuyt PM, Bonsel GJ, van Someren EJ, de Bie RM, Merkus MP, Speelman JD (2000) A comparison of continuous thalamic stimulation and thalamotomy for suppression of severe tremor. N Engl J Med 342: 461–468

Tass, PA (1996) Phase resetting associated with changes of burst shape. J Biol Phys 22: 125–155

Tass PA, Rosenblum MG, Weule J, Kurths J, Pikovsky A, Volkmann J, Schnitzler A, Freund H-J (1998) Detection of $n : m$ phase locking from noisy data: Application to magnetoencephalography. Phys Rev Lett 81: 3291–3294

Tass PA (1999) Phase resetting in medicine and biology – stochastic modelling and data analysis. Springer, Berlin Heidelberg New York

Tass PA (2001a) Effective desynchronization by means of double-pulse phase resetting. Europhys Lett 53(1): 15–21

Tass PA (2001b) Effective desynchronization with a resetting pulse-train followed by a single pulse. Europhys Lett 55(2): 171–177

Tass PA (2001c) Desynchronizing double-pulse phase resetting and application to deep brain stimulation. Biol Cybern 85: 343–354

Tass PA (2002a) Effective desynchronization with a stimulation technique based on soft phase resetting. Europhys Lett 57: 164–170

Tass PA (2002b) Desynchronization of brain rhythms with soft phase-resetting techniques. Biol Cybern 87: 102–115

Tass PA (2002c) Stimulus-locked transient phase dynamics, synchronization and desynchronization of two oscillators. Europhys Lett 59: 199–205

Tass PA (2002d) Effective desynchronization with bipolar double pulse stimulation. Phys Rev E 66: art. no. 036226

Volkmann J, Joliot M, Mogilner A, Ioannides AA, Lado F, Fazzini E, Ribary U, Llinás R (1996) Central motor loop oscillations in parkinsonian resting tremor revealed by magnetoencephalography. Neurology 46: 1359–1370

Wielepp JP, Burgunder JM, Pohle T, Ritter EP, Kinser JA, Krauss JK (2001) Deactivation of thalamocortical activity is responsible for suppression of parkinsonian tremor by thalamic stimulation: a 99mTc-ECD SPECT study. Clin Neurol Neurosurg 103: 228–231

Wunderlin A, Haken H (1975) Scaling theory for nonequilibrium systems. Z Phys B 21: 393–401